

Dynamic Response of Strain Rate Dependent Glass/Epoxy Composite Beams Using Finite Difference Method

M. M. Shokrieh, A. Karamnejad

Abstract—This paper deals with a numerical analysis of the transient response of composite beams with strain rate dependent mechanical properties by use of a finite difference method. The equations of motion based on Timoshenko beam theory are derived. The geometric nonlinearity effects are taken into account with von Kármán large deflection theory. The finite difference method in conjunction with Newmark average acceleration method is applied to solve the differential equations. A modified progressive damage model which accounts for strain rate effects is developed based on the material property degradation rules and modified Hashin-type failure criteria and added to the finite difference model. The components of the model are implemented into a computer code in Mathematica 6. Glass/epoxy laminated composite beams with constant and strain rate dependent mechanical properties under dynamic load are analyzed. Effects of strain rate on dynamic response of the beam for various stacking sequences, load and boundary conditions are investigated.

Keywords—Composite beam, Finite difference method, Progressive damage modeling, Strain rate.

I. INTRODUCTION

COMPOSITE materials are being used in many engineering applications due to their high strength-to-weight and stiffness-to-weight ratio. Structural components such as satellite solar panel, turbine blades and aircraft wings can be considered as composite beams. Since these structures are frequently subjected to dynamic loadings, the study of transient behavior of composite beams is of significant importance. Under intense dynamic loads, the structure experiences high strain rates and since the mechanical properties can vary with strain rate, the transient response of the structure will be dependent on strain rate. Moreover, geometrical nonlinearity and transverse shear strains are important in such dynamic analysis.

Soldatos and Eilshakoff [1] presented a third-order shear deformation theory for static and dynamic analysis of an

orthotropic beam which incorporates the effects of transverse shear and normal deformations. Obst and Rakesh [2] studied the nonlinear static and transient response of laminated beams using a one-dimensional finite element formulation based on higher-order displacement model which accounts for geometric nonlinearities and a parabolic shear strain distribution through the thickness. Marur and Kant [3] used higher-order shear-deformable refined theories, based on isoparametric elements, for transient dynamic analysis of symmetric and un-symmetric sandwich and composite beams. Khdeir [4] developed an analytical solution of the classical, first- and third-order laminate beam to study the transient response of antisymmetric cross-ply laminated beams with generalized boundary conditions and for arbitrary loadings. Kant, *et al.* [5] reported an analytical solution to the natural frequency analysis of composites and sandwich beams based on a higher order refined theory. Gong and Lam [6] investigated the transient response of layered composite beams subjected to underwater shock involving the effects of structural damping and stiffness. None of these literatures considers the effects of strain rate.

In this paper, a macro-mechanical approach using finite difference method and progressive damage modeling algorithm which accounts for geometric nonlinearity effects, transverse shear strain effects and the effects of strain rate is presented. Coupled equations of motion for a laminated composite beam based on Timoshenko beam theory are reduced to ordinary differential equations in time domain using finite difference approximations for displacements. Newmark time integration scheme in association with Newton-Raphson iteration method are applied to solve the system of equations. The variations of mechanical properties due to strain rate and failure are taken into account using empirical relations and sudden material property degradation rules, respectively. A computer code in Mathematica 6 is developed to implement the numerical procedures. The effects of strain rate on transient response of composite beams with various stacking sequences, loadings and boundary conditions are presented and discussed.

II. GOVERNING EQUATIONS

Fig. 1 shows a laminated composite beam under transverse load q . The width b is small compared to the length L and transverse load q is assumed to be a function of x only. In such condition, the mid-plane deflection w_0 and mid-plane

M. M. Shokrieh is with mechanical engineering department of Iran University of Science and Technology as a full professor, Composites Research Laboratory, Mechanical engineering department of Iran University of Science and Technology, Narmak, Tehran, 16846-13114, Iran. (phone: 98-21-7720-8127 & 98-21-77240540-50; fax: 98-21-7749-1206 & 98-21-77240488; e-mail: shokrieh@iust.ac.ir).

A. Karamnejad is with mechanical engineering department of Iran University of Science and Technology, Tehran, Iran. (e-mail: amin_karamnejad@yahoo.com).

displacements in x (u_0) and y (v_0) directions are function of x , and all derivatives with respect to y are zero.

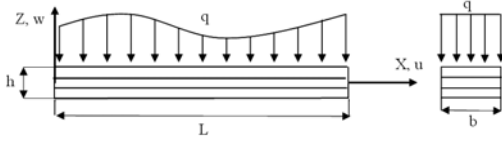


Fig. 1 Laminated composite beam under transverse loading

In addition, in plane forces are zero and as a result in plane displacements (u_0, v_0) are zero. Based on von Kármán theory of plates, nonlinear strain-displacement relations for a composite beam can be written as [7]:

$$\begin{aligned} \varepsilon_{xx} &= 0.5(\partial w_0 / \partial x)^2 + z(\partial \phi_x / \partial x), \gamma_{xz} = \partial w_0 / \partial x + \phi_x, \\ \varepsilon_{yy} &= \gamma_{xy} = \gamma_{yz} = 0 \end{aligned} \quad (1)$$

Where ε_{xx} and ε_{yy} are strains in x and y directions, respectively. γ_{xy}, γ_{xz} and γ_{yz} represent shear strains and ϕ_x is the rotation of the transverse normal about x axis. Stress-strain relations for k th layer are expressed as [7]:

$$\begin{Bmatrix} \sigma_{xx} \\ \sigma_{yy} \\ \sigma_{yz} \\ \sigma_{zx} \\ \sigma_{xy} \end{Bmatrix}^{(k)} = \begin{bmatrix} \bar{Q}_{11} & \bar{Q}_{12} & 0 & 0 & \bar{Q}_{16} \\ \bar{Q}_{12} & \bar{Q}_{22} & 0 & 0 & \bar{Q}_{26} \\ 0 & 0 & 2\bar{Q}_{44} & 2\bar{Q}_{45} & 0 \\ 0 & 0 & 2\bar{Q}_{45} & 2\bar{Q}_{55} & 0 \\ \bar{Q}_{16} & \bar{Q}_{26} & 0 & 0 & 2\bar{Q}_{66} \end{bmatrix}^{(k)} \begin{Bmatrix} \varepsilon_{xx} \\ \varepsilon_{yy} \\ \varepsilon_{yz} \\ \varepsilon_{zx} \\ \varepsilon_{xy} \end{Bmatrix}^{(k)} \quad (2)$$

Where $\bar{Q}_{ij}^{(k)}$ for $i, j=1,2,6$ are plane stress reduced stiffness coefficients and for $i, j=4,5$ denote through the thickness shear stiffness coefficients. $\varepsilon_{yz}, \varepsilon_{zx}$ and ε_{xy} represent tensorial shear strains which are half of the engineering shear strains γ_{yz}, γ_{zx} and γ_{xy} , respectively. $\bar{Q}_{ij}^{(k)}$ can be obtained as follows [7]:

$$[\bar{Q}]^{(k)} = [T^{-1}]^{(k)} [Q]^{(k)} [T]^{(k)} \quad (3)$$

$$[T]^{(k)} = \begin{bmatrix} m^2 & n^2 & 0 & 0 & 2mn \\ n^2 & m^2 & 0 & 0 & -2mn \\ 0 & 0 & m & -n & 0 \\ 0 & 0 & n & m & 0 \\ -mn & mn & 0 & 0 & m^2 - n^2 \end{bmatrix} \quad (4)$$

Where $[T]^{(k)}$ is transformation matrix, $m = \cos \theta_k, n = \sin \theta_k$ and θ_k denotes the angle of fibers with respect to laminate coordinates for k th layer. $Q_{ij}^{(k)}$ can be expressed in terms of engineering constants as follows [7]:

$$\begin{aligned} Q_{11}^{(k)} &= E_{11}^{(k)} / (1 - \nu_{12}^{(k)} \nu_{21}^{(k)}), Q_{12}^{(k)} = \nu_{12}^{(k)} E_{22}^{(k)} / (1 - \nu_{12}^{(k)} \nu_{21}^{(k)}), \\ Q_{22}^{(k)} &= E_{22}^{(k)} / (1 - \nu_{12}^{(k)} \nu_{21}^{(k)}), Q_{66}^{(k)} = G_{12}^{(k)}, Q_{44}^{(k)} = G_{23}^{(k)}, Q_{55}^{(k)} = G_{13}^{(k)} \end{aligned} \quad (5)$$

Where $E_{11}^{(k)}, E_{22}^{(k)}, G_{12}^{(k)}, G_{23}^{(k)}$ and $G_{13}^{(k)}$ are longitudinal, transverse, in plane shear and out of plane shear stiffness values for k th layer, respectively. $\nu_{12}^{(k)}$ and $\nu_{21}^{(k)}$ represent major and minor Poisson's ratios. The constitutive equations for the laminated composite beam with symmetric stacking sequence are given by [7]:

$$\begin{Bmatrix} M_{xx} \\ M_{yy} \\ M_{xy} \end{Bmatrix} = \begin{bmatrix} D_{11} & D_{12} & D_{16} \\ D_{12} & D_{22} & D_{26} \\ D_{16} & D_{26} & D_{66} \end{bmatrix} \begin{Bmatrix} \partial \phi_x / \partial x \\ \partial \phi_y / \partial y \\ \partial \phi_x / \partial y + \partial \phi_y / \partial x \end{Bmatrix} \quad (6)$$

$$\begin{Bmatrix} Q_y \\ Q_x \end{Bmatrix} = K_s \begin{bmatrix} A_{44} & A_{45} \\ A_{45} & A_{55} \end{bmatrix} \begin{Bmatrix} \partial w_0 / \partial y + \phi_y \\ \partial w_0 / \partial x + \phi_x \end{Bmatrix} \quad (7)$$

Where M_{xx}, M_{yy} and M_{xy} are the bending and twisting moments per unit length, respectively. Q_x and Q_y are through the thickness shearing force per unit length. K_s denotes the shear correction coefficient. The recommended shear correction coefficient for a rectangular section is 5/6 [8]. A_{ij} , and D_{ij} are expressed as [7]:

$$D_{ij} = \sum_{k=1}^n \int_{z_k}^{z_{k+1}} \bar{Q}_{ij}^{(k)} z^2 dz \quad i, j = 1, 2, 6 \quad (8)$$

$$A_{ij} = \sum_{k=1}^n \int_{z_k}^{z_{k+1}} \bar{Q}_{ij}^{(k)} dz \quad i, j = 4, 5 \quad (9)$$

Equations of motion based on Timoshenko beam theory for a symmetric laminated composite beam can be obtained by use of dynamic version of the principle of virtual displacements in conjunction with the constitutive equations and the strain-displacement relations as [7]:

$$\begin{aligned} K_s G_{xz}^b h (\partial^2 w_0 / \partial x^2 + \partial \phi_x / \partial x) + b q(x, t) - \hat{I}_0 (\partial^2 w_0 / \partial t^2) &= 0 \\ E_{xx}^b I_{yy} (\partial^2 \phi_x / \partial x^2) - K_s G_{xz}^b h (\partial w_0 / \partial x + \phi_x) - \hat{I}_2 (\partial^2 \phi_x / \partial t^2) &= 0 \end{aligned} \quad (10)$$

Where:

$$E_{xx}^b = 12(D_{11} D_{22} - D_{12} D_{21}) / (D_{22} h^3) \quad (11)$$

$$G_{xz}^b = (A_{44} A_{55} - A_{45} D_{45}) / A_{44} h \quad (12)$$

q is the transverse load (per area) and \hat{I}_i denotes the mass moments of inertia and which can be defined by:

$$(\hat{I}_0, \hat{I}_2) = b \int_{-h/2}^{h/2} (1, z^2) \rho_0 dz \quad (13)$$

Where h and ρ_0 are the laminate thickness and density, respectively. For a rectangular cross section $I_{yy} = 1/12 b h^3$.

III. METHOD OF SOLUTION

Using finite difference approximation for displacement field, coupled partial-differential equations, (10), can be reduced to a set of ordinary differential equations in time domain. Central finite difference equations for first order and second order derivatives of an arbitrary variable f with respect to X can be expressed as:

$$\partial f_{i,j} / \partial X = 1/(2\Delta X)(f_{i+1,j} - f_{i-1,j}) \quad (14)$$

$$\partial^2 f_{i,j} / \partial X^2 = 1/(\Delta X)^2 (f_{i+1,j} - 2f_{i,j} + f_{i-1,j}) \quad (15)$$

Where $f_{i,j}$ denotes the value of f in mesh point (i, j). Finite difference expressions for higher order derivatives can easily be derived from (14) and (15). Using Central finite difference approximations, the differential equations, initial conditions and boundary conditions can be converted into finite difference expressions at the mesh point (i, j). Fig. 2 shows an example finite difference mesh. n represents the number of divisions in x directions.

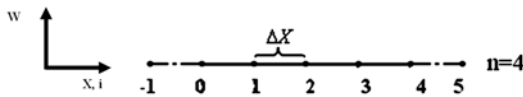


Fig. 2 Finite difference mesh

Assembling these equations for all the mesh points, the matrix form of the equations can be written as:

$$[M]\{\ddot{\Delta}\} + [K]\{\dot{\Delta}\} = \{F\} \quad (16)$$

Where $[K]$ and $[M]$ are the stiffness and mass matrices and $\{\dot{\Delta}\}$ and $\{\ddot{\Delta}\}$ are displacement and acceleration vectors, respectively. The dot superscript denotes a derivative with respect to time. The displacement vector is:

$$\{\Delta\} = \{\{w_i\}, \{\phi_{x_i}\}\}^T \quad i = 1, 2, \dots, n-1 \quad (17)$$

To reduce this set of ordinary differential equations to algebraic equations, we approximate the time derivatives through Newmark time integration scheme. Using Newmark scheme, the fully discretized equations can be expressed as [7]:

$$[\bar{K}(\{\Delta\}_k)]\{\Delta\}_k = \{\bar{F}\}_{k-1,k} \quad (18)$$

$$[\bar{K}(\{\Delta\}_k)] = [K(\{\Delta\}_k)] + a_3[M]_k \quad (19)$$

$$\{\bar{F}\}_{k-1,k} = \{F\}_k + [M]_k \{A\}_{k-1} \quad (20)$$

$$\{A\}_{k-1} = a_3\{\Delta\}_{k-1} + a_4\{\dot{\Delta}\}_{k-1} + a_5\{\ddot{\Delta}\}_{k-1} \quad (21)$$

Equation (18) represents a set of algebraic equations at time t_k . After applying initial and boundary conditions, these equations can be solved using Newton-Raphson iteration method. The new velocity vector $\{\dot{\Delta}\}_k$ and acceleration vector $\{\ddot{\Delta}\}_k$ at the end of k th time step can be computed as [7]:

$$\{\ddot{\Delta}\}_k = a_3(\{\Delta\}_k - \{\Delta\}_{k-1}) - a_4\{\dot{\Delta}\}_{k-1} - a_5\{\ddot{\Delta}\}_{k-1} \quad (22)$$

$$\{\dot{\Delta}\}_k = \{\dot{\Delta}\}_{k-1} + a_2\{\ddot{\Delta}\}_{k-1} + a_1\{\ddot{\Delta}\}_k \quad (23)$$

$$a_1 = \alpha\Delta t, a_2 = (1-\alpha)\Delta t, a_3 = 1/(\beta\Delta t^2), a_4 = a_3\Delta t, a_5 = 1/(2\beta) - 1 \quad (24)$$

Where Δt is the time step and α and β determine the stability and accuracy of the scheme. Here we use the constant-average acceleration method in which $\alpha = 0.5$ and $\beta = 0.5$.

In this work, the response of a composite beam (with length = L) under dynamic load will be investigated under two boundary conditions:

- Simply supported at both edges : at
 $x = 0, L \quad M_{xx} = w = 0$
- Clamped at both edges : $x = 0, L \quad \phi_x = w = 0$

Initial conditions are: at $t = 0 \quad \phi_x = d\phi_x/dt = w = dw/dt = 0$

IV. PROGRESSIVE DAMAGE MODELING

When failure occurs at a point of the laminate, material properties of that point are changed based on material property degradation rules. There are many failure criteria for laminated composites. In this research the modified 2-D Hashin-type failure criteria introduced by Shokrieh [9] are utilized. Failure modes and sudden material property degradation rules for a strain rate dependent composite are expressed as follows:

For the fiber tension:

$$\text{if } \sigma_{11} > 0 \quad (\sigma_{11}/X_t)^2 + (\sigma_{12}/S)^2 = \begin{cases} < 1 & \text{elastic} \\ \geq 1 & \text{failed} \Rightarrow \end{cases} \quad (25)$$

$$[E_1(\dot{\epsilon}_{11}^{(k)}), E_2(\dot{\epsilon}_{22}^{(k)}), G_{12}(\dot{\epsilon}_{12}^{(k)}), \nu_{12}, \nu_{21}] \mapsto [0, 0, 0, 0, 0]$$

$$[X_t(\dot{\epsilon}_{11}^{(k)}), X_c(\dot{\epsilon}_{11}^{(k)}), Y_t(\dot{\epsilon}_{22}^{(k)}), Y_c(\dot{\epsilon}_{22}^{(k)}), S(\dot{\epsilon}_{12}^{(k)})] \mapsto [0, 0, 0, 0, 0]$$

For the fiber compression:

$$\text{if } \sigma_{11} < 0 \quad (\sigma_{11}/X_c)^2 = \begin{cases} < 1 & \text{elastic} \\ \geq 1 & \text{failed} \Rightarrow \end{cases} \quad (26)$$

$$[E_1(\dot{\epsilon}_{11}^{(k)}), E_2(\dot{\epsilon}_{22}^{(k)}), G_{12}(\dot{\epsilon}_{12}^{(k)}), \nu_{12}, \nu_{21}] \mapsto [0, 0, 0, 0, 0]$$

$$[X_t(\dot{\epsilon}_{11}^{(k)}), X_c(\dot{\epsilon}_{11}^{(k)}), Y_t(\dot{\epsilon}_{22}^{(k)}), Y_c(\dot{\epsilon}_{22}^{(k)}), S(\dot{\epsilon}_{12}^{(k)})] \mapsto [0, 0, 0, 0, 0]$$

For the fiber-matrix shearing:

$$\text{if } \sigma_{11} < 0 \quad (\sigma_{11}/X_c)^2 + (\sigma_{12}/S)^2 = \begin{cases} < 1 & \text{elastic} \\ \geq 1 & \text{failed} \Rightarrow \end{cases}$$

$$\begin{aligned}
 & [E_1(\dot{\varepsilon}_{11}^{(k)}), E_2(\dot{\varepsilon}_{22}^{(k)}), G_{12}(\dot{\varepsilon}_{12}^{(k)}), \nu_{12}, \nu_{21}] \mapsto \\
 & [E_1(\dot{\varepsilon}_{11}^{(k+1)}), E_2(\dot{\varepsilon}_{22}^{(k+1)}), 0, 0, 0] \\
 & [X_t(\dot{\varepsilon}_{11}^{(k)}), X_c(\dot{\varepsilon}_{11}^{(k)}), Y_t(\dot{\varepsilon}_{22}^{(k)}), Y_c(\dot{\varepsilon}_{22}^{(k)}), S(\dot{\varepsilon}_{12}^{(k)})] \mapsto \\
 & [X_t(\dot{\varepsilon}_{11}^{(k+1)}), X_c(\dot{\varepsilon}_{11}^{(k+1)}), Y_t(\dot{\varepsilon}_{22}^{(k+1)}), Y_c(\dot{\varepsilon}_{22}^{(k+1)}), 0]
 \end{aligned} \quad (27)$$

For the matrix tension:

$$\text{if } \sigma_{22} > 0 \quad (\sigma_{22}/Y_t)^2 + (\sigma_{12}/S)^2 = \begin{cases} < 1 & \text{elastic} \\ \geq 1 & \text{failed} \Rightarrow \end{cases}$$

$$\begin{aligned}
 & [E_1(\dot{\varepsilon}_{11}^{(k)}), E_2(\dot{\varepsilon}_{22}^{(k)}), G_{12}(\dot{\varepsilon}_{12}^{(k)}), \nu_{12}, \nu_{21}] \mapsto \\
 & [E_1(\dot{\varepsilon}_{11}^{(k+1)}), 0, G_{12}(\dot{\varepsilon}_{12}^{(k+1)}), \nu_{12}, 0] \\
 & [X_t(\dot{\varepsilon}_{11}^{(k)}), X_c(\dot{\varepsilon}_{11}^{(k)}), Y_t(\dot{\varepsilon}_{22}^{(k)}), Y_c(\dot{\varepsilon}_{22}^{(k)}), S(\dot{\varepsilon}_{12}^{(k)})] \mapsto \\
 & [X_t(\dot{\varepsilon}_{11}^{(k+1)}), X_c(\dot{\varepsilon}_{11}^{(k+1)}), 0, Y_c(\dot{\varepsilon}_{22}^{(k+1)}), S(\dot{\varepsilon}_{12}^{(k+1)})]
 \end{aligned} \quad (28)$$

For the matrix compression:

$$\text{if } \sigma_{22} < 0 \quad (\sigma_{22}/Y_c)^2 + (\sigma_{12}/S)^2 = \begin{cases} < 1 & \text{elastic} \\ \geq 1 & \text{failed} \Rightarrow \end{cases}$$

$$\begin{aligned}
 & [E_1(\dot{\varepsilon}_{11}^{(k)}), E_2(\dot{\varepsilon}_{22}^{(k)}), G_{12}(\dot{\varepsilon}_{12}^{(k)}), \nu_{12}, \nu_{21}] \mapsto \\
 & [E_1(\dot{\varepsilon}_{11}^{(k+1)}), 0, G_{12}(\dot{\varepsilon}_{12}^{(k+1)}), \nu_{12}, 0] \\
 & [X_t(\dot{\varepsilon}_{11}^{(k)}), X_c(\dot{\varepsilon}_{11}^{(k)}), Y_t(\dot{\varepsilon}_{22}^{(k)}), Y_c(\dot{\varepsilon}_{22}^{(k)}), S(\dot{\varepsilon}_{12}^{(k)})] \mapsto \\
 & [X_t(\dot{\varepsilon}_{11}^{(k+1)}), X_c(\dot{\varepsilon}_{11}^{(k+1)}), Y_t(\dot{\varepsilon}_{22}^{(k+1)}), 0, S(\dot{\varepsilon}_{12}^{(k+1)})]
 \end{aligned} \quad (29)$$

Where σ_{11} , is the stress of the lamina in fibers direction, σ_{22} is the stress of the lamina in the transverse direction to the fibers and σ_{12} is the in-plane shear stress of the lamina, X_t , X_c , Y_t , Y_c and S are tensile strength of fibers, compressive strength of fibers, tensile strength in transverse direction to the fibers, compressive strength in the transverse direction to the fibers and in plane shear strength, respectively. $\dot{\varepsilon}_{11}^{(k)}$, $\dot{\varepsilon}_{22}^{(k)}$ and $\dot{\varepsilon}_{12}^{(k)}$ are strain rate in fibers direction, strain rate in the transverse direction to the fibers and shear strain rate at k th time step, respectively, which can be obtained as:

$$\dot{\varepsilon}_{ij}^{(k)} = |(\varepsilon_{ij}^{(k)} - \varepsilon_{ij}^{(k-1)}) / \Delta t| \quad (30)$$

σ_{11} , σ_{22} and σ_{12} for n th layer can be calculated from:

$$\begin{Bmatrix} \sigma_{11} \\ \sigma_{22} \\ \sigma_{12} \end{Bmatrix}^{(n)} = \begin{bmatrix} m^2 & n^2 & -2mn \\ n^2 & m^2 & 2mn \\ -mn & mn & m^2 - n^2 \end{bmatrix}^{(n)} \begin{Bmatrix} \sigma_{xx} \\ \sigma_{yy} \\ \sigma_{xy} \end{Bmatrix}^{(n)} \quad (31)$$

Shokrieh and Omidi [10-12] have characterized the effect of strain rate on mechanical properties of unidirectional glass/epoxy using a servo-hydraulic apparatus at varying strain rates, ranging from 0.001 s^{-1} - 100 s^{-1} . In their study, mechanical properties are plotted versus logarithms of strain rate and the data are fitted through a regression function defined by [10-12]:

$$M(\dot{\varepsilon}) = \alpha + \beta \dot{\varepsilon}^\gamma \quad (32)$$

Where, M and $\dot{\varepsilon}$ are the mechanical property and strain rate, respectively. α , β and γ are the material constants. Table I shows α , β and γ values for various mechanical properties of glass/epoxy composites. A computer program based on aforementioned problem formulation has been developed in Mathematica 6.

TABLE I
MATERIAL CONSTANTS IN REGRESSION FUNCTION FOR MECHANICAL PROPERTIES [10-12]

Stiffness (GPa)	E_{11}	E_{22}	G_{12}		
α	37.243	10.037	4.919		
β	1.139	0.437	-0.9408		
γ	0.276	0.2624	0.0545		
Strength (GPa)	X_t	X_c	Y_t	Y_c	S
α	788.1	243.5	43.45	109.9	31.32
β	7.72	316.2	13.09	0.110	15.66
γ	0.886	0.087	0.131	1.278	0.0863

$\rho = 2100 \text{ kg/m}^3$ $\nu_{12} = 0.237$

V. NUMERICAL RESULTS

A. Verification of computer code

Firstly, in order to validate the computer code, results are compared to those of obtained from ABAQUS finite element software. A simply supported glass/epoxy composite beam with stacking sequence $[0]_s$ under uniform step load with the amplitude $q=0.4 \text{ MPa}$ is considered. From Table I static material properties are obtained as ($\dot{\varepsilon} \approx 0$): $E_{11}=37.243 \text{ GPa}$, $E_{22}=10.037 \text{ GPa}$, $G_{12}=G_{13}=4.919 \text{ GPa}$. The beam dimensions are $L=200 \text{ mm}$, $h=16 \text{ mm}$ and $b=20 \text{ mm}$. In this verification study, effects of strain rate on material properties have not been taken into account and no failure occurs under loading. Fig.3 shows the comparison of deflection at the center of the beam (W) obtaining from computer code and ABAQUS. A good agreement is found in Fig. 3 between the two methods.

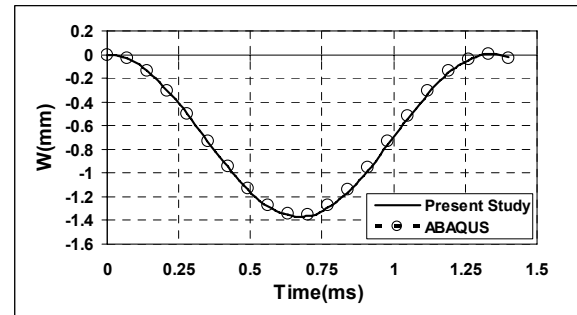


Fig.3 Comparison of center deflection of beam

B. The effect of strain rate

To investigate the strain rate effects, glass/epoxy composite beams under transverse uniform triangular pressure $P=P_{max} (1-t/t_f)$ are studied by use of two material models:

- *Material model a*: Mechanical properties are constant and obtained from static material tests. In here static mechanical properties of glass/epoxy composites are used.
- *Material model b*: Mechanical properties are strain rate dependent and calculated from (32).

Variation of longitudinal strain rate ($\dot{\epsilon}_{11}$) with time at the center of a $[0]_s$ clamped beam with dimensions $L=200\text{ mm}$, $b=20\text{ mm}$ and $h=16\text{ mm}$ under triangular load with $P_{max}=10\text{ MPa}$ and $t_f=1.4\text{ ms}$ is shown in Fig. 4. It can be observed from this figure that the composite beam is exposed to strain rate values higher than 100 s^{-1} . However, as seen before, (32) and material constants given in Table I are valid for strain rates ranging from 0.001 s^{-1} - 100 s^{-1} . Karim [13] and Wang, *et al.* [14] have considered polymer composites by use of a visco-elastic model consisting of an elastic element connected in parallel with a generalized Maxwell model. The stress-strain relationship for the visco-elastic model under constant strain rate $\dot{\epsilon}_{ij}$ can be expressed as [13]:

$$\sigma_{ij} = E_{ij}\epsilon_{ij} + \dot{\epsilon}_{ij} \sum_{k=1}^n \eta_k^{(ij)} \left(1 - \text{Exp}(-\epsilon_{ij} E_k^{(ij)} / \dot{\epsilon}_{ij} \eta_k^{(ij)}) \right) \quad i, j = 1, 2 \quad (33)$$

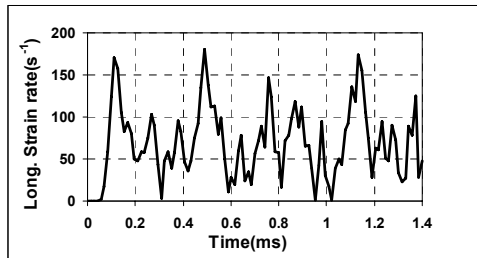


Fig. 4 Variation of longitudinal strain rate with time at the center of the clamped beam

Where E_{ij} is quasi-static stiffness, $E_k^{(ij)}$ and $\eta_k^{(ij)}$ are k th elastic element constant and k th damping element constant, respectively. Nonlinear regression analysis is used to find visco-elastic model parameters by fitting (33) to data obtained from stiffness and strength empirical relations at strain rates ranging from 0.001 s^{-1} - 100 s^{-1} . The visco-elastic model parameters for $n=3$ in longitudinal ($i=j=1$) and transverse ($i=j=2$) directions are given in Table II. From Table I it is obvious that shear stiffness decreases with strain rate ($\beta < 0$) and as a result calculated visco-elastic parameters in shear direction are negative. This implies that the visco-elastic model can not be used to describe shear behavior for the present composite material.

TABLE II
VISCO-ELASTIC MODEL PARAMETERS IN LONGITUDINAL AND TRANSVERSE DIRECTIONS

Longitudinal direction					
$E_1^{(11)}$	$E_2^{(11)}$	$E_3^{(11)}$	$\eta_1^{(11)}$	$\eta_2^{(11)}$	$\eta_3^{(11)}$
0.384824	2.3938	0.62314	0.1567	0.00035	0.004476
Transverse direction					
$E_1^{(22)}$	$E_2^{(22)}$	$E_3^{(22)}$	$\eta_1^{(22)}$	$\eta_2^{(22)}$	$\eta_3^{(22)}$
0.155086	0.0068	0.835001	1.3E-5	0.22935	0.000175

Prediction of longitudinal and transverse stiffness and strength values using the visco-elastic model and empirical equations at strain rate 200 s^{-1} are given in Table III. As seen in Table III the material properties calculated using the visco-elastic model are almost in agreement with those calculated using empirical relations. This indicates that empirical equations can be used to estimate longitudinal and transverse stiffness and strength values at strain rates higher than 100 s^{-1} . The variation of shear stiffness and strength with logarithm of strain rate is approximately linear. According to Okoli and Smith [15], this linear relationship implies that extrapolation of low strain rate data to region of high strain rate data is possible. Moreover, the logarithm of $200 (=2.3)$ is close to that of 100 . Therefore, in this research shear stiffness and strength empirical equations for strain rates higher than 100 s^{-1} (up to 200 s^{-1}) are used.

Results for the deflection of the center of a $400\text{ mm} \times 20\text{ mm} \times 16\text{ mm}$ simply supported and clamped composite beam with $[0]_s$ stacking sequence subjected to triangular load with $P_{max}=10\text{ MPa}$ and $t_f=1.4\text{ ms}$, are presented for material model *a* and material model *b* in Figs. 5 and 6, respectively.

TABLE III
COMPARISON OF STRENGTHS AND STIFFNESS VALUES OBTAINED USING VISCO-ELASTIC MODEL AND EMPIRICAL EQUATION AT 200 s^{-1}

Stiffness(GPa)	Visco-elastic model	Empirical equation
E_{11}	40.6	42.16
E_{22}	11.8	11.14
Strength(MPa)	Visco-elastic model	Empirical equation
X_t	1197	1632
X_c	746.2	746
Y_t	63.27	69.7
Y_c	294	206

As shown in these figures, for both boundary conditions, the maximum center deflection obtained from the material model *a* is larger than that of obtained from the material model *b*. This is due to the fact that, the magnitudes of stiffness in material model *b* increase by increasing the strain rate. Therefore, the material model *a* which has constant mechanical properties behaves softer than the material model *b*.

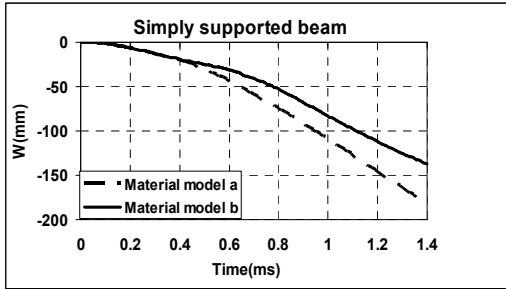


Fig.5 Comparison of center deflection for simply supported beam (Under triangular load: $P_{max}=10MPa, t_f=1.4ms$)

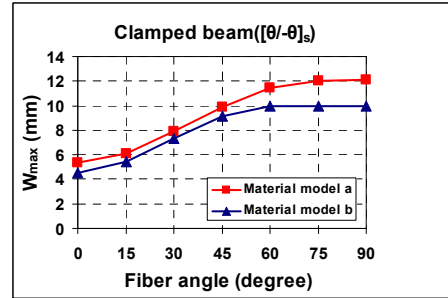


Fig. 8 Maximum center deflection for clamped beam (Under triangular load: $P_{max}=0.8MPa, t_f=1.4ms$)

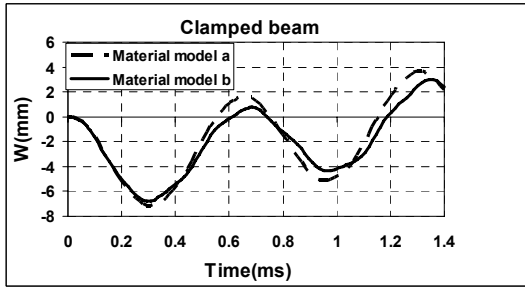


Fig.6 Comparison of center deflection for clamped beam (Under triangular load: $P_{max}=10MPa, t_f=1.4ms$)

The effect of stacking sequence are investigated by material models *a* and *b* for lamination scheme $[\theta/-\theta]_s$ in which $\theta=0^\circ, 15^\circ, 30^\circ, 45^\circ, 60^\circ, 75^\circ$ and 90° . Fig.7 depicts the time history of center deflection for $400\text{ mm}\times 20\text{ mm}\times 16\text{ mm}$ clamped beams which are exposed to triangular load with $P_{max}=0.8\text{ MPa}$ and $t_f=1.4\text{ ms}$ using material models *a* and *b* for $\theta=0^\circ, 45^\circ$ and 90° . The variation of maximum deflection (W_{max}) with fiber angle (θ) is illustrated in Fig. 8. As shown in Figs. 7 and 8, the maximum center deflection increases with fiber orientation angle and reaches its maximum value at $\theta=90^\circ$. It can be seen that the trends for material model *a* and *b* are the same. It is also clear that for all stacking sequences the maximum center deflection obtained using the material model *a* is larger than that of the material model *b*.

In order to study the effect of peak pressure (P_{max}), a $200\text{ mm}\times 20\text{ mm}\times 16\text{ mm}$ clamped glass/epoxy composite beam with the stacking sequence $[0]_s$ subjected to triangular load with $P_{max}=4, 6, 8, 10$ and 12 MPa and $t_f=1.4\text{ ms}$ is analyzed.

Fig. 9 represents time history of center deflection of the beam under peak loads with $P_{max}=2$ and 12 MPa . As seen in Fig. 9, the difference between results obtaining from material model *a* and *b* is greater for $P_{max}=12\text{ MPa}$. The variation of maximum deflection (W_{max}) with peak load (P_{max}) is shown in Fig. 10. From this figure, it is obvious that the maximum center deflection as well as the difference between results obtained using material model *a* and *b* increase with the magnitude of the peak pressure. This is due to the fact that the strain rate magnitude increases with an increase in P_{max} and as a result, the difference between rate dependent mechanical properties of the material model *b* and constant mechanical properties of material model *a* increases.

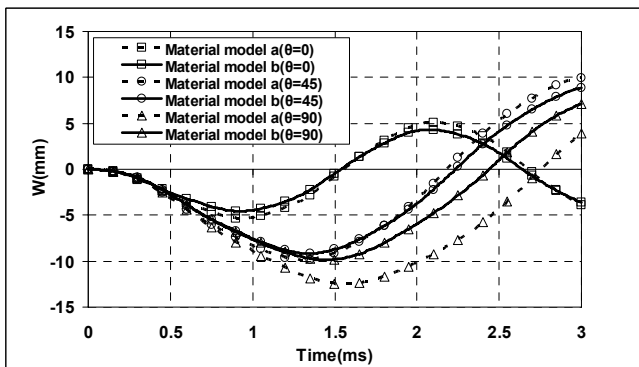


Fig.7 Center deflection history of clamped beams with lamination scheme $[\theta/-\theta]_s$ for $\theta=0^\circ, 45^\circ, 90^\circ$

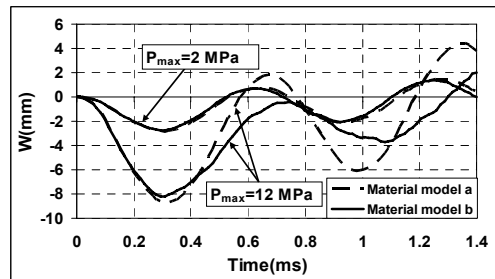


Fig. 9 History of center deflection for clamped beam

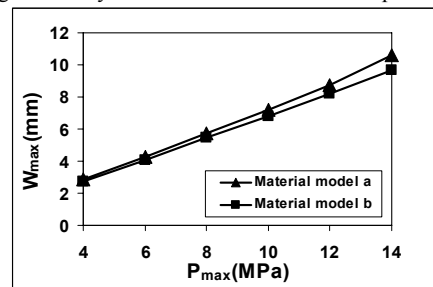


Fig. 10 Variation of maximum deflection with peak pressure

VI. CONCLUSION

In the present study, a finite difference model which accounts for geometric nonlinearity, shear transverse strain is presented, based on Timoshenko beam theory. Sudden material degradation rules, Hashin-type failure criteria and

empirical relations which present longitudinal, transverse and shear magnitudes of strength and stiffness in terms of strain rate are used to develop a strain rate dependent progressive damage model. Finite difference model in association with the progressive damage model are programmed in a Mathematica computer code. In order to investigate the strain rate effects on the dynamic response of the composite, a clamped glass/epoxy composite beam subjected to a dynamic load is considered. Results for the material model *a*, in which the mechanical properties are constant, and the material model *b* which has strain rate dependent mechanical properties, are compared for various stacking sequences and load magnitudes. The results obtained from the present research are summarized as follows:

- Longitudinal and transverse behaviors of a glass/epoxy lamina (which is used in the present study) can be described using a visco-elastic model, consisting of an elastic element connected in parallel with a generalized Maxwell model, but this model can not be used for glass/epoxy composites under shear loading.
- The maximum deflection obtained at the center of the beam, using the material model *a* (with constant material properties) is larger than that obtained using the material model *b* (with strain rate dependent material properties).
- The effect of stacking sequence on the maximum deflection of the center of the composite beam is the same for both material models *a* and *b*. the maximum center deflection for a $[\theta/-\theta]_s$ stacking sequence is obtained when θ is equal to 90° .
- The maximum deflection and the difference between results obtained using material models *a* and *b* increase by increasing the magnitude of the load.

REFERENCES

- [1] K. P. Soldatos and I. Elishakoff, "A transverse shear and normal deformable orthotropic beam theory", *Journal of Sound and Vibration*, vol. 154, no. 3, pp. 528–33, June 1992.
- [2] A. W. Obst and R. K. Kapania, "Nonlinear static and transient finite element analysis of laminated beams", *Composite Engineering*, vol. 2, no. 5-7, pp. 375-389, Feb. 1992.
- [3] S. R. Marur and T. Kant, "On the performance of higher order theories for transient dynamic analysis of sandwich and composite beams", *Composites & Structures*, vol. 65, no. 5, pp. 741-759, Dec. 1997.
- [4] A. A. Khedeir, "Dynamic response of antisymmetric cross-ply laminated composite beams with arbitrary boundary conditions", *International Journal of Engineering Science*, vol. 34, no. 1, pp. 9-19, Jan. 1996.
- [5] T. Kant, S. R. Marur and G. S. Rao, "Analytical solution to the dynamic analysis of laminated beams using higher order refined theory", *Composite Structures*, vol. 40, no.1, pp. 1-9, Dec. 1997.
- [6] S. W. Gong and K. Y. Lam, "Analysis of layered composite beam to underwater shock including structural damping and stiffness effects", *Shock and Vibration*, vol. 9, no. 6, pp. 283-291, 2002.
- [7] J. N. Reddy, *Mechanics of Laminated Composite Plates and Shells: Theory and Analysis*, second ed., CRC Press, Boca Raton, FL, 2004, pp. 109-197.
- [8] *LS-DYNA 971 Keyword User's Manual*, Livermore Software Technology Corporation, California, USA, 2006, pp.1840-1841.
- [9] M. M. Shokrieh, "Progressive Fatigue Damage Modeling of Composite Materials", Ph.D. thesis, Dept. Mech. Eng., McGill Univ., Montreal, Canada, 1996.
- [10] M. M. Shokrieh and M. J. Omid, "Tension behavior of unidirectional glass/epoxy composites under different strain rates", *Composite Structures*, vol. 88, no. 4, pp. 595-601, May 2009.
- [11] M. M. Shokrieh and M. J. Omid, "Compressive response of glass-fiber reinforced polymeric composites to increasing compressive strain rates", *Composite Structures*, vol. 89, no. 4, pp. 517-523, Aug. 2009.
- [12] M. M. Shokrieh and M. J. Omid, "Investigation of strain rate effects on in-plane shear properties of glass/epoxy composites", *Composite Structures*, vol. 91, no. 1, pp. 95-102, Nov. 2009.
- [13] M. R. Karim, "Constitutive Modeling and Failure Criteria of Carbon-Fiber Reinforced Polymers under High Strain rates", Ph.D. thesis, The Graduate Faculty of The University of Akron, USA, 2005.
- [14] W. Wang, G. Makarov and R. A. Shenoi, "An analytical model for assessing strain rate sensitivity of unidirectional composite laminates", *Composite Structures*, vol.69, no.1, pp. 45-54, June 2005.
- [15] O. I. Okoli and G. F. Smith, "High strain rate characterization of a glass/epoxy composite", *Journal of Composites Technology & Research*, vol. 22, no. 1, pp. 3-11, Jan. 2000.